GEOPHYSICAL RESEARCH LETTERS, VOL. 34, L08703, doi:10.1029/2006GL028502, 2007

Implications of changes in the atmospheric circulation on the detection of regional surface air temperature trends

Qigang Wu[1] and David J. Karoly[1]

Received 18 October 2006; revised 26 February 2007; accepted 6 March 2007; published 19 April 2007.

[1] Previous studies have shown that observed significant warming trends in surface air temperature (SAT) consistent with the response to anthropogenic forcing are detected at scales on the order of 500 km in many regions of the globe. However, regional SAT trends project strongly on the dominant natural atmospheric circulation modes, such as the Arctic Oscillation (AO) and the hemispheric Pacific-North America (PNA)-like patterns. The warming associated with the changes of atmospheric circulation is not well simulated in current coupled climate models. In this study, we explore the influence of the exclusion of warming related to changes of the atmospheric circulation on the detection of a regional response to combined anthropogenic and natural forcings. We compare observed SAT trends over the second half of the 20th century with those simulated in response to natural and anthropogenic climate forcings in a suite of six current coupled general circulation models. Control runs from these models are used to provide estimates of the internal variability of trends. We find that the detection of the regional response to combined anthropogenic and natural forcing is robust to the exclusion of warming related to changes of the atmospheric circulation considered here. **Citation:** Wu, Q., and D. J. Karoly (2007), Implications of changes in the atmospheric circulation on the detection of regional surface air temperature trends, *Geophys. Res. Lett.*, *34*, L08703, doi:10.1029/2006GL028502.

1. Introduction

[2] During the past two decades, many global and large-scale studies using various space-time detection methods have identified the significant impact of anthropogenic forcing on the 20th century climate (see the assessment by *Mitchell et al.* [2001] for the Intergovernmental Panel on Climate Change (IPCC) Third Assessment, and the review by *International Ad Hoc Detection and Attribution Group* [2005]). Recently, two analyses have extended these studies to regional scales. *Karoly and Wu* [2005] considered observed warming trends at individual 5° × 5° cells over 30, 50 and 100 year periods ending in 2002 and showed that, over a large fraction of the globe, the significant warming trends could not be explained by natural variability estimated by climate models. They also showed that the regional warming in the 2nd half of the 20th century was not consistent with the response to natural external forcing. *Knutson et al.* [2006] found evidence for an emergent anthropogenic warming signal over many regions of the globe during the second half of the 20th century in an assessment of surface temperature trends in individual grid cells using the GFDL CM2 coupled models.

[3] The impact of the changes in the atmospheric circulation on regional climate has been recognized in a number of studies. For example, variations of the annular modes [*Thompson and Wallace*, 1998] have been reported to explain much of observed warming trend over the middle latitudes of Northern Hemisphere (NH) in winter [*Thompson et al.*, 2000]. In the NH winter, the PNA -like pattern has also been shown to explain much of observed warming trend in both Northern America and Eurasia [*Wu and Straus*, 2004; *Quadrelli and Wallace*, 2004]. In the Southern Hemisphere (SH), the similarity between the Antarctic Oscillation (AAO) and the warming trends in higher latitudes have been reported [*Hurrell and van Loon*, 1994; *Chen and Yen*, 1997; *Randel and Wu*, 1999]. However, SAT trends associated with those atmospheric circulation modes may not be well represented in the GCMs because current GCMs might underestimate the internal variability or fail to capture the magnitude of the response of the atmospheric circulation to increasing anthropogenic greenhouse and aerosols [*Gillett et al.*, 2005; *Gillett*, 2005].

[4] *Gillett et al.* [2000] and *Zwiers and Zhang* [2003] found that the detection of global and large-scale anthropogenic warming in surface temperatures over the second half of the 20th century is still robust after the AO-related warming is excluded. The main purpose here is to investigate the influence of the changes of the atmospheric circulation on the detection of regional SAT trends. We consider the local significance of warming trends at individual 5° × 5° grid boxes after removing the contribution from observed and modeled changes in atmospheric circulation. The field significance test by *Karoly and Wu* [2005] is applied to determine whether the fraction of grid boxes that show locally significant trends is still greater than would be expected by chance after the warming related to the AO, AAO and PNA-like patterns is excluded. In addition, the observed residual trends are compared with the corresponding multimodel averaged response to assess whether the observed residual trends are consistent with the response to changes in major anthropogenic and natural forcing factors.

2. Datasets

[5] The observed SAT trends are calculated from a new dataset of monthly mean surface temperature data for 1951–2000 and 1971–2000 on a 5° latitude–longitude grid (HadCRUT3v) [*Brohan et al.*, 2006]. Natural variability of linear SAT trends is calculated from the pre-industrial control runs and the forced SAT trends are calculated from the 20th century historical simulations (20C3M) generated for

[1]School of Meteorology, University of Oklahoma, Norman, Oklahoma, USA.

0094-8276/07/2006GL028502

Table 1. Observed and Simulated PNA-Like Modes[a]

Observed/Model	NCEP/NCAR	GFDL_CM2.0	GFDL_CM2.1	CCSM 3	PCM	MIROC	MRI-CGCM2
Correlation		0.92	0.81	0.85	0.58	0.92	0.84
Linear trend	1.63	0.31	0.16	−0.05	0.35	0.19	0.15

[a]The first row lists the spatial correlation of the hemispheric PNA-like modes (defined as the second EOF of monthly SLP anomalies north of 20°N over the period 1951–2000) for six GCMs with the observed pattern from NCEP/NCAR reanalysis; the 2nd row gives the linear trends (per 50 yr) of the corresponding second principal component for the observations and each model.

the Fourth Assessment of the IPCC (AR4). A total of 3100 years of pre-industrial control simulations from six models: GFDL-CM2.0, GFDL-CM2.1, CCSM3, PCM, MIROC3.2 (medres) and MRI-CGCM2.3.2, is used to estimate the natural variability of trends. The 20C3M simulations used here are also from these six models. The forcing in the 20C3M simulations from the above six models includes at least the changes in the major anthropogenic and natural forcings: greenhouse gases, the direct sulfate aerosol effect, stratospheric ozone, volcanic aerosol and solar irradiance. Some of the models also include indirect sulfate aerosol effects, black carbon aerosols and land use changes. Additional information on the above six models and assumed forcing is available at http://www-pcmdi.llnl.gov/ipcc/model_documentation/ipcc_model_documentation.php. In total, 26 individual 20C3M simulations were used. Since the 20C3M simulations generally finished in 1999 or 2000, we focus our analysis in the 2nd half of the 20th century. Only regions with data available throughout most of the 1951–2000 and 1971–2000 periods are considered, with grid boxes having more than 66% of years available included in the trend analysis. The data from the model grids are at a higher horizontal resolution than the observed datasets and have been interpolated onto the observed 5° grid for the analysis.

[6] Observed atmospheric circulation index values for the AO and PNA-like patterns during 1951–2000 are from the NCEP-NCAR Reanalysis [*Kalnay et al.*, 1996] obtained from the NOAA's Climate Diagnostics Center. Empirical orthogonal function (EOF) analysis is applied to the monthly mean sea level pressure (SLP) anomalies north of 20°N for the period 1951–2000. In the EOF analysis, area weighting is accomplished by multiplying SLP by the square root of the cosine of latitude before computing the covariance matrix. The leading two EOFs of SLP are readily identifiable as being the AO and PNA-like patterns respectively [*Wu and Straus*, 2004; *Quadrelli and Wallace*, 2004]. The corresponding two standardized principal component (PC) time series are defined as the AO and PNA-like mode index. Here we ignore the possible uncertainties to the index values induced by the NCEP-NCAR reanalysis that used a frozen state-of-the-art global data assimilation system to fill in gaps. Reliability of the trends in the NCEP-NCAR reanalysis in the SH midlatitude and high latitude have been questioned [*Randel and Wu*, 1999; *Marshall*, 2003]. Here the AAO index for the period of 1951–2000 is taken from *Marshall* [2003] (available at http://jisao.washington.edu/aao/slp/). As given by *Marshall* [2003], the leading PC is first obtained from the EOF analysis of SLP anomalies for the grid boxes south of 20°S during 1979–2005. Such PC is then correlated with global SLP anomalies and the resulting correlation map is projected onto the data to produce a time series for AAO for the period of 1948–2005. More details are given by *Marshall* [2003]. The SAT trend independent of these atmospheric circulation modes is estimated at each grid box by three steps: (1) regressing monthly values of that grid point's SAT time series onto the three circulation indices simultaneously; (2) calculating the residual monthly SAT after removing variations correlated with these circulation modes; and then (3) calculating the linear trend from the monthly residuals. Note that in step 1, changes in SAT only have the circulation index as a descriptor. But in reality there would also be other factors influencing the SAT at 500-km scales, such as global forcing and internal variability. By only regressing the index out, which may or may not be correlated with the forcing, we can find how big the influence associated with these indices is on the SAT, but part of the change in indices may be a forced response. The model SAT trend of response to the historical forcing independent of the simulated circulation modes is defined in the same way. Also the same method is used to remove the trends in SAT associated with three circulation modes in the control simulations.

[7] *Miller et al.* [2006] have shown that the six models in this study simulated realistic annular patterns and interannual variance during the late 20th century, and that the AO changes in these models are of smaller amplitudes than the upward trend observed since 1950 (also see *Gillett* [2005] and others). The observed hemispheric PNA-like pattern [see *Wu and Straus*, 2004, Figure 1b] has embedded within it the PNA pattern of *Wallace and Gutzler* [1981], an important regional pattern, and one which is thought to play a role in explaining the observed correlations between Atlantic and Pacific SLP, as discussed by *Ambaum et al.* [2001] and *Wallace and Thompson* [2002]. Six models here have simulated PNA-like modes well, but the associated trends are much less than observed (see Table 1). The results on PNA-like mode changes, together with what has been found for the AO changes by Gillett et al. and Miller et al., imply that only part of the observed circulation trends is found as a forced response in current GCMs.

3. Results

3.1. Comparison of Observed SAT Trends With Natural Variability of Trends

[8] The internal variability of 50 yr (30 yr) linear trends at each grid box is calculated from the 50 yr (30 yr) segments of the total 3100 years of control simulations concatenated together from six GCMs since only a short section of control is available in each case. The climate drift of control simulations at each grid box is removed separately for each model. To increase the sample size, we calculate the natural variability of the 50 yr linear trends from overlapping segments starting 25 years apart (15 yrs

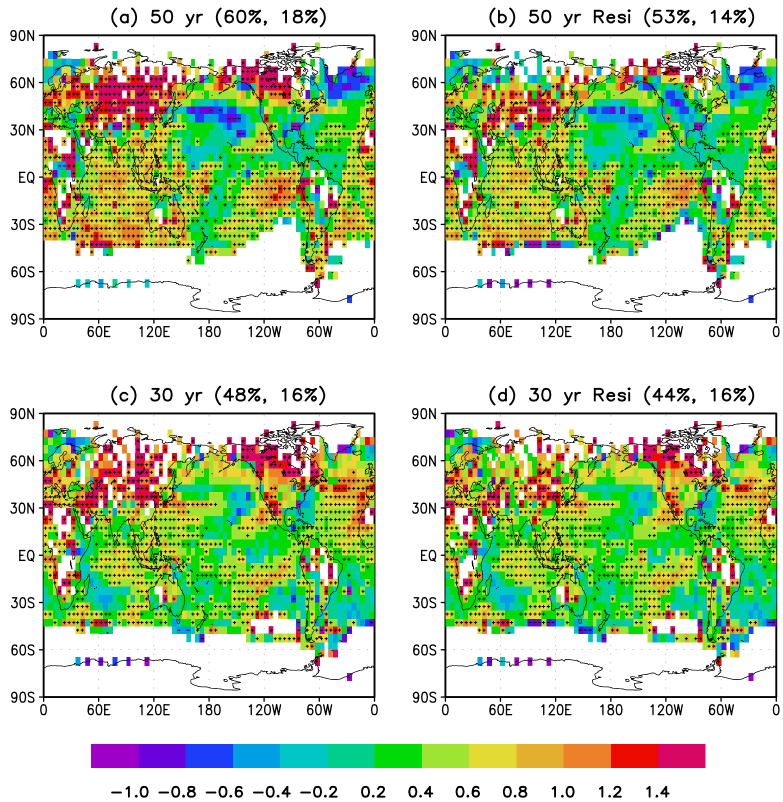

Figure 1. Observed trends in surface temperature over the periods (a, b) 1951–2000 and (c, d) 1971–2000. Trends in Figures 1a and 1c are calculated from the original HadCRUT3v dataset, and the corresponding residual trends in Figures 1b and 1d are calculated after the AO, PNA-like, and AAO related components are removed. Plus (minus) symbols mark individual grid boxes where the observed trends are significantly larger (smaller) than zero at the 95% level using a one-sided test. Above each map is the fraction of grid boxes with significant warming trends and the 95th percentile for the distribution of fractions for significant warming trends that could occur due to natural internal climate variability.

for 30-yr trends) in the control simulations. We have about 120 and 200 realizations of estimated linear trends for 50 and 30 yr periods respectively. The temperature trends from the control runs are approximately normally distributed and the standard deviation of this distribution is used as the measure of the natural variability of linear trends. At each grid-box, we apply a one-sided local significance test to identify whether the observed SAT trend is significantly different from zero at the 95% level. The range of fractions of grid boxes with significant trends that could occur due to internal variability is determined by the field significance test based on the approach of *Livezey and Chen* [1983]. On average, in a stationary climate, only 5% of the grid boxes are expected to show warming trends significant at the 95% level due to random variability alone. As there is large spatial coherence of low-frequency variations of SAT, a much larger fraction of significant warming trend might occur by chance. For 50-yr trends, we consider the linear trends at each grid box from the control simulation and determine the fraction of grid boxes that show locally significant warming trends. This is repeated 120 times (200 times for 30-yr trends) to determine the distribution of grid box fractions with significant warming that could occur due to internal climate variations.

[9] Figure 1 shows the pattern of observed trends in color, with the significant warming (cooling) trends marked with a + (−) symbol. About 60% and 48% of the individual grid boxes with sufficient observational data show significant warming trends over the period 1951–2000, and 1971–2000 respectively. Although the expected value is 5%, the 95th percentile for the distribution of fractions for significant 50-yr trends is 18%, and 16% for 30-yr trends. The fraction of grid boxes with significant observed warming trends is large for both trend periods and much greater than the range of trend fractions that could be expected due to internal climate variations. This is consistent with results by *Karoly and Wu* [2005], who compared the SAT trends in HadCRUT2v dataset with natural variability of trends estimated from control simulations from three individual GCMs.

[10] In the NH, the circulation changes have induced a significant part of the warming. After removing the contributions from these circulation patterns, corresponding residual trends for two periods in Figure 1 still show the same patterns as their corresponding overall trends, but they are much weaker in the NH mid-latitude. In the SH, the circulation patterns have also caused some of the trends in SAT. For the period 1951–2000 (1971–2000), the circulation modes contribute more than 20% of the total SAT trends for about 10% (13%) of grid boxes, 10% to 20% of the total trends for about 56% (17%) of grid boxes in the SH. For the residual trends, about 53% and 44% of the

Table 2. Global Fractions of Significant Regional Trends

Periods	Significant Trends[a]		Significantly Different From 20C3M Trend[b]	
	1951–2000	1971–2000	1951–2000	1971–2000
Observed (annual)	60% (18%)	48% (16%)	29% (24%)	13% (22%)
Residual (annual)	53% (14%)	44% (16%)	20% (26%)	10% (23%)
Observed (Nov.–Apr.)	53% (16%)	41% (15%)	23% (21%)	10% (22%)
Residual (Nov.–Apr.)	43% (13%)	34% (13%)	14% (22%)	9% (23%)

[a]Fraction of grid boxes over the globe with observed annual and NH cold season (Nov. to Apr.) linear warming trends and their corresponding residual trends (after AO, AAO, and PNA-like mode related components are removed) locally significant at the 95% level over 50 and 30 yr intervals. The number in parentheses is the result of a field significance test to determine the largest value of this fraction due to natural climate variability. It represents at least the 95% significance level for the field significance of the fraction of significant grid boxes.

[b]Same as in "Significant Trends" columns, but for the fraction of grid boxes where the observed and residual trends are significantly different from the ensemble-mean multimodel averaged response to historical forcing, using a two-sided test at the 90% level.

individual grid boxes with sufficient observational data show significant warming trends over the 50 and 30 yr periods respectively. The fraction of grid boxes with significant observed warming trends for each sample period is still much greater than the range of trend fractions that could be expected due to internal climate variations. At any one of these individual grid boxes with a significant warming trend, we can say that we have detected a significant warming trend that is very unlikely to be due to natural internal climate variations alone.

[11] It may be argued that the SAT trend pattern projects more strongly on the atmospheric circulation modes in NH winter than for the annual time period. We compare observed SAT trends in the NH cold season (November to April) for the two different periods to the corresponding natural variability of linear trends. As given in Table 2, about 53% and 41% of grid boxes with sufficient observational data show significant warming trends over the 50 and 30 yr periods for the cold season observed SAT trends, while the fractions are reduced to 43% and 34% for the cold season residual trends, and both are still much greater than the range of trend fractions that could be expected due to internal climate variations.

3.2. Comparison of Observed SAT Trends With the Model Trends

[12] Next, we assess whether the observed warming trend at each of the grid boxes is locally consistent with the multimodel-averaged trend of simulated response to historical forcings for the 20th century. The purpose here is to examine whether changes in SAT shown in Figure 1 are consistent with the response to combined anthropogenic and natural causes. It has been shown that the use of multiple model signals helps to reduce the uncertainties in the climate signal detection and attribution [*Gillett et al.*, 2002]. We conduct a two-side test to determine whether the difference between the observed warming trend and the multimodel averaged warming trend from the 20C3M simulations is significantly different from zero at each grid box. Figure 2 shows the averaged GCM warming trends from 26 realizations of six models over the 50 and 30 yr periods and their corresponding residual trends after the AO, PNA-like and AAO related components are removed. Grid boxes where the modeled warming trend is significantly greater (smaller) than the observed trend are shown by a plus (minus) symbol. The fraction of the grid boxes where the observed trend is not consistent with the all-forcing simulations is much smaller than in Figure 1: 29% for the trend over 1951–2000 and 13% for 1971–2000. Also shown in brackets in Figure 2 are the 95th percentiles of the distribution of fractions of grid boxes that give significantly different trends due to internal variability (estimated from the control simulations). The fraction of grid boxes where the observed trends over 50 yr are not consistent with the model all-forcing response is outside the range that can be explained by internal variability. There are regions with model trend significantly smaller than observed, indicating that the multi-model averaged response to both anthropogenic and natural forcing still cannot explain the observed trend over this period. After the AO, AAO and PNA related trends are removed, the residual trends over the 50 yr period are consistent with the ensemble mean multimodel averaged response to all forcings, as 20% of grid boxes where the observed trends are not consistent with the multimodel averaged trends can be explained by internal climate variations. For the 1971–2000 period, the observed trends and the residual trends are both consistent with the multimodel averaged response to all forcings.

[13] Similar results are found when we examine the consistency between the NH cold season observed trend and the multimodel-averaged response to historical forcings at each grid box (see Table 2). For 1951–2000, the fraction of the grid boxes where the observed wintertime trend is not consistent with the all-forcing simulations is 23%, but such fraction of grid boxes is reduced to 14% for the residual trends.

4. Summary

[14] Attention has been drawn to potential problems in climate change detection and prediction if the response of atmospheric circulation regimes to external forcing is unrealistically simulated in the climate model used [*Shindell et al.*, 1999; *Corti et al.*, 1999; *Palmer*, 1999]. For example, if the model underestimates the change in the AO, but the observed AO response looks like the model non-AO anthropogenic response, then the observed AO change may project onto the fingerprint of anthropogenic climate change. In a formal detection study [*Allen and Stott*, 2003], the modeled anthropogenic response may be scaled up, thus leading to an overestimate of the amplitude of the anthropogenic signal.

[15] In this study, we have shown that the observed warming trends over the last 50 and 30 years of the 20th century at individual grid boxes are significantly different

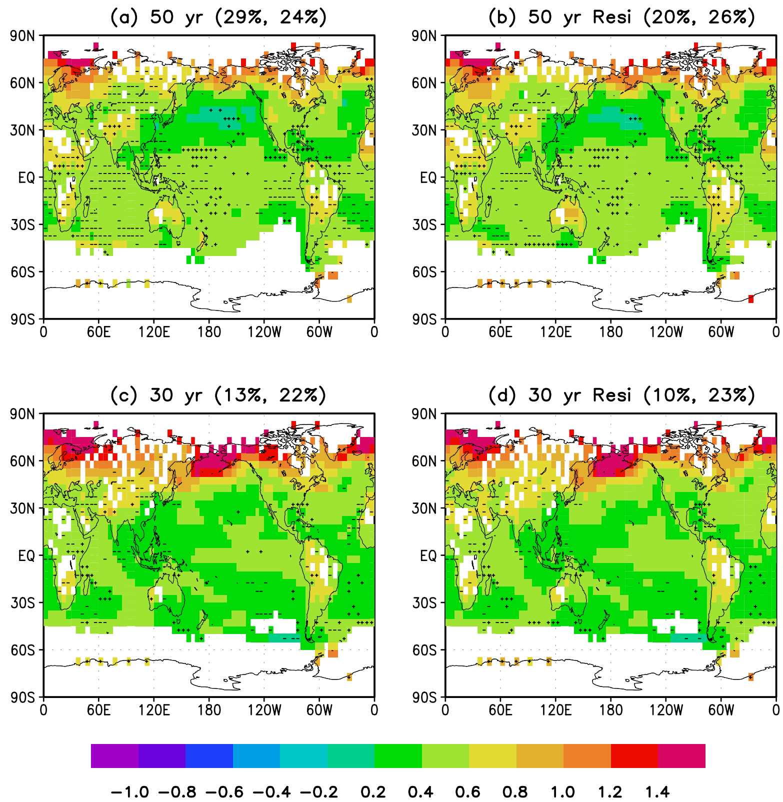

Figure 2. Ensemble mean multimodel averaged trends in surface temperature in response to major anthropogenic and natural forcings from six GCMs over the periods (a) 1951–2000, and (c) 1971–2000. (b, d) The corresponding residual trends are calculated after the AO, PNA-like pattern, and AAO components are removed over the 50 and 30 yr intervals. Plus (minus) symbols mark individual grid boxes where the model trends are significantly larger (smaller) than the observed trends at the 90% level using a two-sided test. Above each map is the fraction of grid boxes with significantly different trends than observed and the 95th percentile for the distribution of such fractions that could occur due to natural internal climate variability.

from zero at large fractions of the grid boxes over the globe even after the AO, PNA-like mode and AAO related components are removed. These fractions are much too large to be explained as a chance occurrence due to internal climate variations. In addition, the observed trends over the 50 yr period are not consistent with the ensemble mean multimodel response to major anthropogenic and natural forcings. However, the observed residual trends over the 50 yr period are consistent with the model response, which indicates the impact of atmosphere circulation on the attribution of temperature trends. Note that we have not assessed the pattern of observed warming at the 500-km scale and are not saying that spatial variations in the warming at the 500-km scale can be detected. In practice, we have shown that the observed warming trend is larger than can be explained by internal variability at the 500-km scale even after the trends induced by the main atmospheric circulation modes are removed. Our results show that there is an important component of the regional SAT warming to major anthropogenic and natural forcing which is distinct from that associated with the dominant atmospheric circulation modes, such as the AO, AAO and PNA-like modes.

[16] **Acknowledgments.** QW is supported by a Gary Comer Science and Education Foundation Postdoctoral Fellowship. This research has been support by NSF grant ATM-0555326. We wish to acknowledge the international modeling groups for providing their data for analysis, and the Program for Climate Model Diagnosis and Intercomparsion (PCMDI) for collecting and archiving the model data.

References

Allen, M. R., and P. A. Stott (2003), Estimating signal amplitudes in optimal fingerprinting, part I: Theory, *Clim. Dyn.*, *21*, 477–491.
Ambaum, M. P., B. J. Hoskins, and D. B. Stephenson (2001), Arctic Oscillation or North Atlantic Oscillation?, *J. Clim.*, *14*, 3495–3507.
Brohan, P., J. J. Kennedy, I. Harris, S. F. B. Tett, and P. D. Jones (2006), Uncertainty estimates in regional and global observed temperature changes: A new data set from 1850, *J. Geophys. Res.*, *111*, D12106, doi:10.1029/2005JD006548.
Chen, T.-C., and M.-C. Yen (1997), Interdecadal variation of the Southern Hemisphere circulation, *J. Clim.*, *10*, 805–812.
Corti, S., F. Molteni, and T. N. Palmer (1999), Signature of recent climate change in frequencies of natural atmospheric circulation regimes, *Nature*, *398*, 799–802.
Gillett, N. P. (2005), *Northern Hemisphere circulation*, *437*, 496.
Gillett, N. P., G. C. Hegerl, M. R. Allen, and P. A. Stott (2000), Implications of changes in the Northern Hemisphere circulation for the detection of anthropogenic climate change, *Geophys. Res. Lett.*, *27*(7), 993–996, doi:10.1029/1999GL010981.
Gillett, N. P., F. W. Zwiers, A. J. Weaver, G. C. Hegerl, M. R. Allen, and P. A. Stott (2002), Detecting anthropogenic influence with a multi-model ensemble, *Geophys. Res. Lett.*, *29*(20), 1970, doi:10.1029/2002GL015836.
Gillett, N. P., R. J. Allan, and T. J. Ansell (2005), Detection of external influence on sea level pressure with a multi-model ensemble, *Geophys. Res. Lett.*, *32*, L19714, doi:10.1029/2005GL023640.
Hurrell, J. W., and H. van Loon (1994), A modulation of the atmospheric annual cycle in the Southern Hemisphere, *Tellus, Ser. A*, *46*, 325–338.

International Ad Hoc Detection and Attribution Group (2005), Detecting and attributing external influences on the climate system: A review of recent advances, *J. Clim.*, *18*, 1291–1314.

Kalnay, E., et al. (1996), The NCEP/NCAR 40-year reanalysis project, *Bull. Am. Meteorol. Soc.*, *77*, 437–472.

Karoly, D. J., and Q. Wu (2005), Detection of regional surface temperature trends, *J. Clim.*, *18*, 4337–4343.

Knutson, T. R., T. L. Delworth, K. W. Dixon, I. M. Held, J. Lu, V. Ramaswamy, M. D. Schwarzkopf, G. Stenchikov, and R. J. Stouffer (2006), Assessment of twentieth-century regional surface temperature trends using the GFDL CM2 coupled models, *J. Clim.*, *19*, 1624–1651.

Livezey, R. E., and W. Y. Chen (1983), Statistical field significance and its determination by Monte Carlo techniques, *Mon. Weather Rev.*, *111*, 46–49.

Marshall, G. J. (2003), Trends in the Southern Annular Mode from observations and reanalyses, *J. Clim.*, *16*, 4134–4143.

Miller, R. L., G. A. Schmidt, and D. T. Shindell (2006), Forced annular variations in the 20th century Intergovernmental Panel on Climate Change Fourth Assessment Report models, *J. Geophys. Res.*, *111*, D18101, doi:10.1029/2005JD006323.

Mitchell, J. F. B., D. J. Karoly, M. R. Allen, G. Hegerl, F. Zwiers, and J. Marengo (2001), Detection of climate change and attribution of causes, in *Climate Change 2001: The Scientific Basis*, edited by J. T. Houghton et al., pp. 695–738, Cambridge Univ. Press, New York.

Palmer, T. P. (1999), A nonlinear dynamical perspective on climate prediction, *J. Clim.*, *12*, 575–591.

Quadrelli, R., and J. M. Wallace (2004), Varied expressions of the hemispheric circulation observed in association with contrasting polarities of prescribed patterns of variability, *J. Clim.*, *17*, 4245–4253.

Randel, W. J., and F. Wu (1999), Cooling of the Arctic and Antarctic polar stratospheres due to ozone depletion, *J. Clim.*, *12*, 1467–1479.

Shindell, D. T., R. L. Miller, G. A. Schmidt, and L. Pandolfo (1999), Simulation of recent northern winter climate trends by greenhouse-gas forcing, *Nature*, *399*, 452–455.

Thompson, D. W. J., and J. M. Wallace (1998), The Arctic Oscillation signature in the wintertime geopotential height and temperature fields, *Geophys. Res. Lett.*, *25*(9), 1297–1300.

Thompson, D. W. J., J. M. Wallace, and G. C. Hegerl (2000), Annular modes in the extratropical circulation. part II: Trends, *J. Clim.*, *13*, 1018–1036.

Wallace, J. M., and D. S. Gutzler (1981), Teleconnections in the geopotential height field during the Northern Hemisphere winter, *Mon. Weather Rev.*, *109*, 784–812.

Wallace, J. M., and D. W. J. Thompson (2002), The Pacific center of action of the Northern Hemisphere annular mode: Real or artifact?, *J. Clim.*, *15*, 1987–1991.

Wu, Q., and D. M. Straus (2004), AO, COWL, and observed climate trends, *J. Clim.*, *17*, 2139–2156.

Zwiers, F. W., and X. Zhang (2003), Toward regional-scale climate change detection, *J. Clim.*, *16*, 793–797.

D. J. Karoly and Q. Wu, School of Meteorology, University of Oklahoma, 120 David L. Boren Boulevard, Suite 5900, Norman, OK 73072, USA. (wuqig@rossby.metr.ou.edu)